Energy and Buildings 86 (2015) 573–588

Contents lists available at ScienceDirect

Energy and Buildings

journal homepage: www.elsevier.com/locate/enbuild

The influence of hospital ward design on resilience to heat waves: An exploration using distributed lag models

C.R. Iddon [a,b], T.C. Mills [c], R. Giridharan [d], K.J. Lomas [a,*]

[a] Building Energy Research Group School of Civil and Building Engineering, Loughborough University, LE11 3TU, UK
[b] SE Controls Lancaster House, Wellington Crescent, Fradley Park, Lichfield, Staffordshire WS13 8RZ, UK
[c] School of Business and Economics, Loughborough University, LE11 3TU, UK
[d] Kent School of Architecture, University of Kent, Canterbury CT2 7NZ, UK

ARTICLE INFO

Article history:
Received 1 May 2014
Received in revised form
25 September 2014
Accepted 26 September 2014
Available online 29 October 2014

Keywords:
Heatwave
Overheating risk
Distributed lag models
Thermal modelling
Hospitals
Resilliance
Prediction
Forecasting

ABSTRACT

Distributed lag models (DLMs) to predict future internal temperatures have been developed using the hourly weather data and the internal temperatures recorded in eleven spaces on two UK National Health Service (NHS) hospital sites. The ward spaces were in five buildings of very different type and age. In all the DLMs, the best prediction of internal temperature was obtained using three exogenous drivers, previous internal temperature, external temperature and solar radiation. DLMs were sensitive to the buildings' differences in orientation, thermal mass and shading and were validated by comparing the predictions with the internal temperatures recorded in the summer of 2012. The results were encouraging, with both modelled and recorded data showing good correlation. To understand the resilience of the spaces to heat waves, the DLMs were fed with weather data recorded during the hot summer of 2006. The Nightingale wards and traditional masonry wards showed remarkable resilience to the hot weather. In contrast, light-weight modular buildings were predicted to overheat dangerously. By recording internal temperatures for a short period, DLMs might be created that can forecast future temperatures in many other types of naturally ventilated or mixed-mode buildings as a means of assessing overheating risk.

1. Introduction

In populated areas around the globe, and irrespective of local climate, periods of prolonged and uncharacteristically high external temperature (often referred to as 'heat waves' though debate over the specific definition of such events remain) correlate to increases in localised mortality rates. The heat wave in Quebec 2010 saw a 33% increase in daily death rates [1], and in Brisbane, where people are well accustomed to hot weather, significant increases in mortality were reported during heat waves between 1996 and 2005 [2]. Estimates of over 50,000 extra deaths have been recorded for the Europe-wide heat wave of 2003, of which 22,080 excess deaths were reported in England, Wales, France, Italy and Portugal [3]. Episodes of prolonged hot weather have been demonstrated to increase mortality in certain vulnerable demographics, particularly the over 80s, and to increase in the number of cardiovascular deaths in individuals aged 45 years or older [4] whilst in Suzhou, China, no significant modifying effect by gender, age or educational level was observed on temperature–mortality relationship [5].

The Intergovernmental Panel on Climate Change (IPCC) reports that since 1950 there is a medium confidence that there has been a consistent increase in Warm Spell Duration Index (WSDI),[1] an indicator of the number and frequency of heat wave events, in Northern Europe [6–8]. It is likely that heat waves will be longer and more intense in the future due to a warming climate, though there is some dependency on the parameterisation choice used in models to predict these events [6,9]. Regardless of their predicted frequency and intensity, heat waves will continue to occur and this, in conjunction with evidence from past events, has focussed efforts on the means and methods to reduce the risks of mortality during hot weather.

In England, the Department for Health publishes a yearly heat wave plan [10]. Studies on heat waves in London have demonstrated that although mortality increases during heat waves, hospital admissions do not increase significantly, suggesting that

* Corresponding author. Tel.: +44 01509 222615.
E-mail address: k.l.lomas@lboro.ac.uk (K.J. Lomas).

[1] Warm Spell Duration Index (WSDI): fraction of days per year or season which belong to periods of at least 6 days at which consecutively T_{max} > q90, where q90 gives the climatological 90%-quartile of T_{max} for that day.

http://dx.doi.org/10.1016/j.enbuild.2014.09.053

the most vulnerable groups are the elderly living alone or with limited social contact, and the heat wave plans rightly focus particular attention on these demographics [11].

Hospitals must be resilient to heat waves as they house people with chronic medical conditions who are thus vulnerable to prolonged high temperature. Proposed measures to reduce mortality risks to patients during heat wave events, include maintaining 'cool' zones [10,12]. Kravchenko et al., in an American study, recommend controlling the internal environment and provision of 'cool' zones with air conditioning, however the National Health Service (NHS) faces a challenge: how to deliver safe environments in a changing climate whilst meeting ambitious carbon reduction targets. Widespread use of air-conditioning is unlikely to meet both criteria [13,14].

Very few hospital wards in the UK are air-conditioned; instead the internal temperature is maintained by natural or mechanical ventilation. The summertime internal temperatures in 125 such spaces, of which 97 were wards, located on four hospital sites, (Addenbrooke's, Cambridge; Glenfield, Leicester; St. Albans; and Bradford Royal Infirmary), were measured as part of the UK project, Design and Delivery of Robust Hospital Environments in a Changing Climate (DeDeRHECC), the largest known UK survey of hospital temperatures. These data were then used to calibrate dynamic thermal models and the likely overheating during heat wave events predicted [14–17]. Thermally lightweight construction was predicted to increase the risk of overheating. Refurbishment options to reduce overheating risk *and* reduce energy demands were explored.

This paper capitalises on the DeDeRHECC data but develops empirical models for wards through statistical analysis of measured internal and external temperatures. This approach, which avoided the errors and uncertainties associated with thermal model calibration, led to the creation of a unique distributed lag model (DLMs) for each hospital ward. The DLMs were created using data collected during the summer of 2011 and validated against data from the summer of 2012. The models were then used to predict the resilience of wards in buildings of different type to an extremely hot summer; the Europe-wide heat wave of 2006.

1.1. Modelling internal temperature

Previous studies, such as the DeDeRHECC project, have tended to focus on the development of dynamic thermal models as a way to understand the characteristic response of room temperature and to provide a means of future forecasting. Such models use a building physics approach, in which the salient thermo-physical properties of the building are exposed to past or future boundary conditions. Many of the thermo-physical features, and the details of the boundary conditions, are unknown and so assumptions must be made. To aid this process, measurements sometimes are used to provide data against which to 'calibrate' the model in order to improve the fit between predicted and measured parameters, such as internal air temperature e.g. [14,15,17]. There are however many model inputs for which assumptions must be made and the final set of inputs, although 'valid' based on the limited knowledge of the system in question, are just one possible set of inputs that could be selected. Models also embed simplifications, internal heat gains are estimated and specified as simple, repeating daily schedules and real-world events can often be ignored or grossly simplified, for example occupant window opening. Thus even 'calibrated' models are inherently limited and assumption choice may be biased by knowing the recorded data to which the model should align; the model therefore loses impartiality [18,19].

An alternative approach to understanding the factors that drive internal temperatures in a space is to develop purely empirical models which consider the dynamic heat balance of a space which, at a point in time, can be considered as: heat of a system = heat into a system – heat lost from the system. The recorded internal temperatures provide a snapshot of the dynamic heat energy balance at work in the space. Comparison of the recorded internal temperature at the $t_{=0}$ and $t_{=-1}$ time-points allows the elucidation of whether the heat energy into the space is greater or less than heat lost from the space over a time period such as an hour. This can provide an insight into the magnitude of energy into, and out of a system on an hourly basis, such that; if energy into the system is greater than that leaving the system, the internal temperature will increase with respect to the temperature at $t_{=-1}$.

The difficulty with such an analysis lies in the myriad processes that affect the space heat balance. These include, but are not limited to, heat supplied to, or lost from a space via the ventilation system, through air leakage, from room occupants, through window openings, by fabric conduction, by solar radiation, from lighting and small power sources, and, in winter, the heating system. Even a computer thermal model that has undergone the most rigorous calibration will still not accurately reflect measured temperatures as there is so much that will never be known with regard to transient influences on the internal temperature.

Time series analysis has often been employed with temperature data sets, not least because regular diurnal and seasonal trends can be readily modelled by such analysis. Models have been generated to: predict external air and solar radiation events [20]; predict the response of internal temperature to changes in outside temperature [21]; predict internal temperature for HVAC control systems [22]; to estimate building energy performance by robust regression [23]; and to model climate change [24]. Similar principles are used in this paper to create a model that can reproduce the inherent features of the internal temperature profiles recorded in hospital wards.

This paper reports work in which a novel time series model was developed to predict the internal temperature at any time, t_0, based upon the internal temperature in preceding hours and the driving exogenous effects of external dry bulb temperature, external global solar irradiance and external solar irradiance incident on the plane of the building. Comparing the diurnal internal temperature profiles in several spaces as recorded in the summer of 2011, revealed a relationship with room orientation. Using this as a starting point, a distributed lag model (DLM) of internal temperature was created for each space based on the measured hourly external weather conditions, and the internal temperatures recorded in each space.

1.2. Modelled spaces

As part of the DeDeRHECC project, temperatures were recorded at hourly intervals for between 6 months and 3 years, in 97 wards, in 9 hospital buildings, on four sites: Bradford Royal infirmary, Leicester Glenfield, Addenbrookes Hospital Cambridge, and St Albans Hospital. This paper focuses on 11 hospital wards in five buildings on the Bradford and St Albans sites. These provide examples of a variety of architectural forms and construction types: a traditional (c1930s), thermally heavyweight, Nightingale building [14,25]; a very modern (2008), thermally lightweight, modular building; and three 1960s–1970s buildings, two towers – the matchbox of the 'matchbox on a muffin' building type [17] and a masonry slab building (Table 1). The buildings, with their roughly north-south axis orientation, test the ability of the time series analysis to detect the influence of ward orientation, east or west, on space temperatures. Further information regarding the spaces monitored can be found in the electronic appendix.

Temperature loggers, Hobo type U12-001, were used to record the temperatures at hourly intervals, however, the location of each

Table 1
Building types, locations and descriptions ofwardstaken as representative for the building.

Location	Ward type	Building details	Space Ref[a]	Space details
Bradford RI	Nightingale	Built c1927–1937 Walls – stone, c.500 mm thick, comprising 150 mm stone outer skin and 350–400 mm inner skin with some rubble infill Windows – thermally broken aluminium-framed double glazed units Ventilation – natural ventilation, opening windows	BNi-W	Twin bed ward facing due west 270° N Volume, 60 m^3 Ground floor
Bradford RI	Modular	Built 2008 Walls – lightweight insulated panels *U*-value 0.2 Wm^2 K	BMo-E	Single bed rooms Facing due east 90° N Volume, 42 m^3 Ground floor
		Windows – double glazed, toughened, low e soft coat, *U*-value of 1.2 W/m^2 K Ventilation – mechanical ventilated, supply into rooms, extract via fabric and dedicated extract ducts in toilet areas. Circa 4ach. Windows can be opened to provide further ventilation.	BMo-W	Multi-bed wards Facing due west 270° N Volume, 123 m^3 Ground floor
Bradford RI	Maternity Tower Linear Slab Rooms from 'matchbox' element of the 'Matchbox on a Muffin' type	Built c1965–1967 Concrete frame with continuous window ribbon incorporating opaque panels Opaque panels – Gyproc system with insulated cavity Windows – recently replaced double glazed system Ventilation – mechanical ventilated, supply into rooms, extract via fabric and dedicated extract ducts in toilet areas. Circa 4ach. Windows can be opened to provide further ventilation.	BMa-E	Single bed Facing due east 90° N Volume, 35 m^3 m 4th Floor
			BMa-W	Multi-bed ward facing due west 270° N Volume, 150 m^3 4th Floor
St Albans	Moynihan Building Tower Linear Slab Rooms from 'matchbox' element of the 'Matchbox on a Muffin' type	Built circa early 1970s Concrete frame with continuous timber frame ribbon incorporating windows and opaque panels. Opaque panels – painted WBP timber outer sheet with 25 mm thick dense mineral fibre insulation panel bonded to inner face. Windows – single glazed Ventilation – mechanical ventilated, supply into rooms, extract via fabric and dedicated extract ducts in toilet areas. Circa 4ach. Windows can be opened to provide further ventilation.	SMa-E	Multi-bed ward facing south easterly 135° N Volume, 150 m^3 Fifth floor
St Albans	Traditional Masonry slab Runcie Building	Built 1983 Traditional build, 102 mm brickwork outer skin walling, 50 mm cavity air-gap, 50 mm mineral fibre insulation, 100 mm thick medium density blockwork. Windows – timber framed, double glazed Ventilation – mechanical ventilated, supply into rooms, extract via fabric and dedicated extract ducts in toilet areas. Circa 4ach. Windows can be opened to provide further ventilation.	$SMs\text{-}E_{sf}$	Single bed ward facing south easterly, 135° N Volume 30 m^3 2nd floor
			$SMs\text{-}W1_{gf}$ $SMs\text{-}W2_{gf}$ $SMs\text{-}W1_{sf}$ $SMs\text{-}W2_{sf}$	Multi bed ward facing north westerly, 315° N Volume 135 m^3 Ground and 2nd floor

[a] Room coding: B – Bradford, S – St Albans; Ni – Nightingale, Mo – Modular, Ms – Masonry slab, and Ma – Matchbox element of a 'matchbox on a muffin' type; E – East, W – West; gf – ground floor, sf – second floor.

one was heavily constrained by clinical, and other, considerations.[2] The loggers were fixed to the walls in such a way that they could be removed for data downloading and, if necessary, cleaning (for infection control). They were located as far a possible away from heat sources and other thermal stimuli, which would interfere with the attempt to record a mean space temperature. The loggers, which record spot values on the hour, are quoted as being accurate to ±0.35 °C, and in pre-trial testing the installed loggers recorded to within 0.2 K of each other at normal room temperature.

The local meteorological data, hourly external dry bulb temperature, and global horizontal solar irradiance were recorded by local weather stations, Bingley for Bradford and Northolt for St Albans. Weather stations set up local to each hospital, as part of the DeDeRHECC project, were used in the 2012 data set. Values for the solar radiation incident (SRI) on the external plane of the wards were calculated using the procedure described in the appendix text.

Data from 1st May to 30th September 2011 was used to develop the DLM for each ward and data recorded from June to September 2012 to test DLMs' accuracy. Data from other periods is used to illustrate features of the measured data and DLMs' behaviour.

2. Results

2.1. Average diurnal temperature profiles

To appreciate the diurnal temperature profile at each measurement location, the average of all the hourly data at a given hour point collected between 1st May and 30th September 2011 was plotted (i.e. 153 × 24 = 3672 h).

Average daily temperature profiles for the east-facing single bed wards of the modular building (BMo-E) and matchbox tower building (BMa-E), indicate that that these spaces warm in the morning between 06:00 and 09:00 and that in the heavily insulated modular

[2] In general, spaces had two loggers but the data used to generate the models was taken from just one of these because loggers at the back of rooms had a tendency to be affected by direct solar gain. However, whichever sensor (or average of the two) was used, a DLM could be generated.

building (BMo-E) the peak temperature is maintained through the course of the afternoon before cooling around 19:00 h whilst the matchbox ward begins to cool earlier (Fig. 1). In contrast, the west-facing wards (BMo-W, BMa-W and BNi) begin to warm around 12:00 and reach a peak temperature around 18:00–19:00 after which the spaces begin to cool. Generally, the peak temperature of such west-facing wards is higher than in the east facing spaces, but east-facing spaces cool more slowly and therefore spend more time at high temperatures, making them more prone to overheating as defined by the number of hours over a set threshold temperature. The heavyweight Nightingale ward (BNi-W) displays a much smaller diurnal swing in internal temperature (1 K) than the lighter weight matchbox and modular wards (BMa-W, BMo-W); diurnal swing circa 2 K. Similar results, which typify east and west facing wards, were observed in the diurnal profiles recorded in the St. Albans Moynihan Tower and Runcie buildings (results not shown).

Although the average temperatures at each hour illustrate clear differences between the east and west facing rooms, there is, of course, very large variability between the individual hourly values. To better account for this variability, and thus to develop a more robust model of internal temperature variations, the difference in temperatures, Δt, from a 48 h moving average are used to define the ward temperature t_0:

$$\Delta t_0 = t_0 - \left(\frac{\sum_{t=-24}^{23} t}{48} \right) \quad (1)$$

The hourly internal temperature in a single bed ward in the modular building at Bradford (BMo-E) and the 48 h moving average temperature are illustrated in (Fig. 2)

2.2. Impact of solar radiation on internal temperatures

Plotting the monthly average hourly temperature difference from the 48 h mean against the monthly average hourly incident solar radiation incident on the glazing of a ward, demonstrated a co-incidence between the increase in internal temperature and the increase in incident solar radiation (Fig. 3).

During January, where the average monthly solar radiation is low, there is little average diurnal swing in internal room temperature away from the 48 h moving average (Fig. 3A and C). Conversely, in April, the higher incident solar radiation drives up the internal temperatures (Fig. 3B and D) with the west facing ward BMo-W (B) warming in the late afternoon and the east facing ward (BMo-E) warming in the morning (D). Similar plots to those shown in Fig. 3 have been generated for many different months and many wards in all the building types. All these demonstrate the coordination

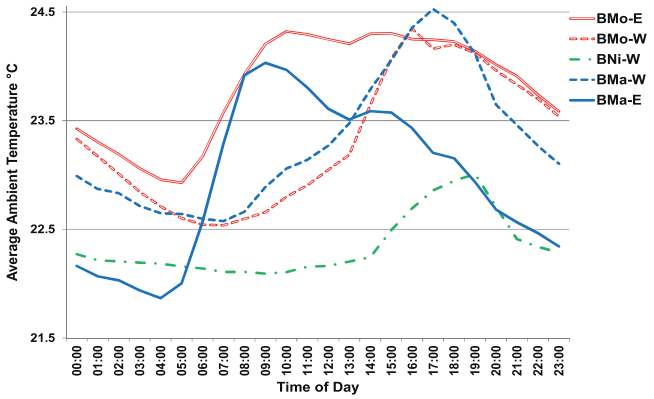

Fig. 1. The hourly average internal temperature during the summer of 2011 in east-facing (BMo-E, BMa-E) and west-facing (BMo-W, BMa-W and BNi-W) wards at Bradford Royal Infirmary. Similar results for other spaces at Bradford Royal Infirmary are given in the electronic appendix.

of increases in internal room temperature with increased incident solar radiation. The plots generated for the 21 months from January 2010 to September 2011 for wards BMa-E, BMa-W, BNi-W, BMo-E and BMo-W have been collated into a video file (Video 01), which can be viewed in the electronic appendix to this paper.

Unexpected results were obtained for the ground floor wards in the masonry slab building at St. Albans (SMs-$W1_{gf}$ and SMs-$W2_{gf}$). In these spaces, the internal temperature was insensitive to the incident solar radiation, yet other west facing wards in the same building showed the expected sensitivity (Fig. 4A and B, cf., respectively, 4C and 4D).

Further investigation (Google imagery and a site visit) revealed that temporary site cabins had been erected just a few metres from the windows on the ground floor wards (Fig. 5A) and Google SketchUp (Now Trimble SketchUp) shadow plots confirmed that the cabins blocked nearly all direct solar radiation into the ground floor wards (Fig. 5B) but not into those on the second floor (Fig. 5C).

Monthly average hourly internal temperature versus incident solar radiation profiles for other monitored spaces (results not shown) provided evidence for localised shading that decreased the internal temperature variations. These observations suggest that solar gains are one of the most significant factors influencing internal temperature. Therefore, any empirical model to predict internal temperature must be sensitive to the influence that the local site topography has on solar heat gains.

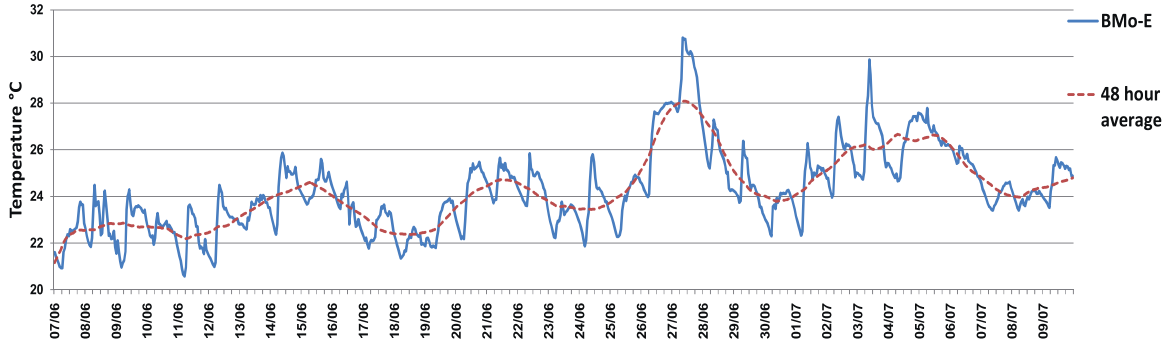

Fig. 2. Hourly internal temperature recorded between 7th June and 9th July 2011, in a single bed ward in the modular building at Bradford Royal Infirmary (BMo-E), showing the 48 h moving average. The 'noise' of the raw temperature data is evident as positive and negative spikes and is due to sudden changes in the space heat balance, due most likely to occupant events (such as opening the windows) or transient heat gains (from solar gain or occupants).

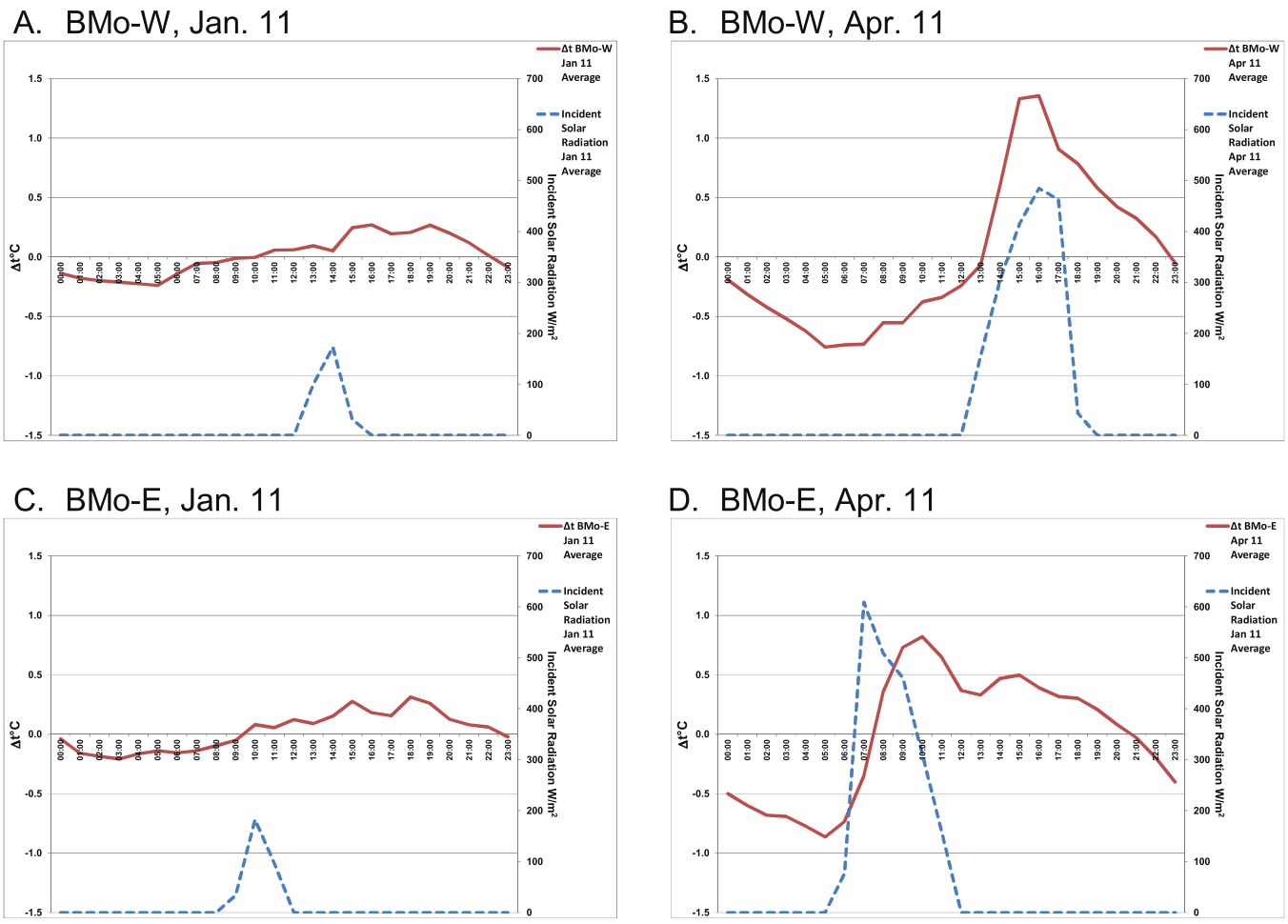

Fig. 3. Graphs showing the monthly diurnal average incident solar radiation (blue dash line) and internal Δt (red solid line) during January and April 2011. Modular multibed ward facing west (BMo-W) during January (A) and April (B). Modular single bed ward facing east (BMo-E) during January (C) and April (D). (For interpretation of the references to color in this figure legend, the reader is referred to the web version of this article.)

2.3. Time series analysis

In light of the suggested correlation between internal temperature and incident solar radiation a time series approach was used to try and create a model that reproduced the recorded response of the internal temperature to three exogenous effects, namely, external dry bulb temperature, global solar irradiance and incident solar radiation.

Denoting the room temperature as T_t, external temperature as T_{ext}, global solar irradiation as S_{global} and incident solar radiation as $S_{incident}$, a distributed lag model (DLM) was developed:

$$T_t = c + \sum_{i=0}^{p} \alpha_i T_{t-1-i} + \sum_{i=0}^{p} \beta_i T_{ext_{t-i}} + \sum_{i=0}^{p} \gamma_i S_{global_{t-i}} + \sum_{i=0}^{p} \delta_i S_{incident_{t-i}} + u_i \quad (2)$$

Herein, u_t is an error term that is assumed to be identically and independently distributed as $N(0, \sigma_u^2)$ and the room temperature at time t is assumed to be a linear function of past lags of itself and current and past lags of the three exogenous variables. This specification is an example of the traditional econometric autoregressive DLM, e.g. [26], in which the order of the lags are selected to ensure that all dynamic effects are accounted for and no autocorrelation remains in the error term.

After some experimentation with the lag structure, using EViews software ([27] EViews, 2013), and by re-expressing variables to facilitate easier interpretation, the following general model was selected[3] as providing an adequate fit for each of the rooms modelled:

$$T_t = c + \alpha_1 T_{t-1} + \alpha_2 T_{t-2} + \alpha_3 T_{t-24} + \beta_0 T_{ext_t} + \beta_1 \nabla T_{ext_t} + (\gamma_0 + \gamma_1) S_{global_t} + \gamma_1 \nabla S_{global_t} + (\delta_0 + \delta_3) S_{incident_t} + \delta_3 \nabla_3 S_{incident_t} + \delta_{23} S_{incident_{t-23}} + \delta_{24} S_{incident_{t-24}} + u_t \quad (3)$$

In this equation regressors have been combined to aid interpretation (essentially level and change effects have been emphasised: generically: $\nabla_k X_t = X_t = X_{t-k}$). T_{ext_t} represents the external temperature at time t in °C; S_{global_t} represents the global horizontal solar radiation at time t in W/m^2; $S_{incident_t}$ represents the solar radiation incident to the façade of the space at time t in W/m^2; T_{t-i} represents the past internal room temperature at time $t-i$ in °C; α, β, γ and δ are the coefficients related to internal temperature, external temperature, global solar radiation and incident solar radiation respectively; and c is a constant.

[3] 'Selected' here means: selected as the best 'general' model to fit all data, to create a model that could be applied to all spaces.

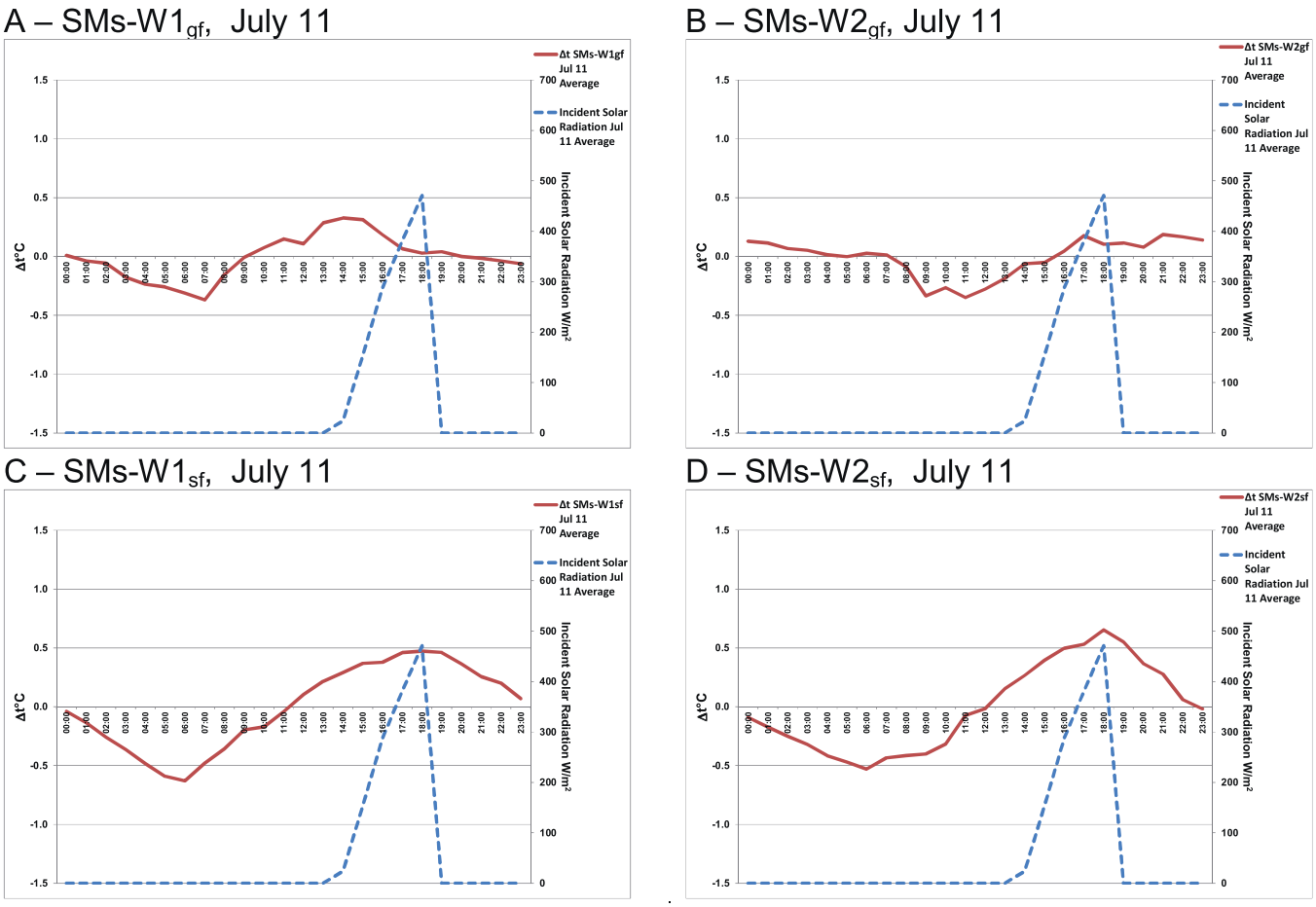

Fig. 4. Graph showing the monthly average hourly incident solar radiation (blue dashed) and average hourly internal temperature difference from the 48 h mean (red solid line) for July 2011. Results are shown for the west facing masonry building at St. Albans: two ground floor north westerly (315° N) facing wards, SMs-W1$_{gf}$, (A) and, SMs-W2$_{gf}$, (B) and two second floor north westerly facing wards, SMs-W1$_{sf}$, (C) and SMs-W2sf,(D). (For interpretation of the references to color in this figure legend, the reader is referred to the web version of this article.)

The form of this DLM suggests that internal temperature at time t depends on the previous internal temperatures (at time $t=-1$, $t=-2$ and $t=-24$), the current and past external temperature (i.e. at $t=0$ and $t=-1$), the current and past global solar radiation (i.e. at $t=0$ and $t=-1$) and the change in global solar radiation (between $t=0$ and $t=-1$) and, finally, the current and past incident solar radiation (at $t=0$, $t=-3$, $t=-23$, $t=-24$) and the change in incident solar radiation (between $t=0$ and $t=-3$). This formulation is discussed in the context of the thermal physics at play in each space in Section 3.

Using the recorded hourly data between 1st May and 30th September 2011, DLMs were created for five wards at Bradford Royal infirmary (Table 2). These five were chosen because they were representative of east and west facing wards of thermally heavyweight Nightingale, 'matchbox on a muffin' and light weight modular construction types. In all five cases the 12 coefficients were precisely determined with a small standard error and were robust to general forms of autocorrelation and heteroskedasticity (Table 2). As indicated by the coefficient of determination, R^2

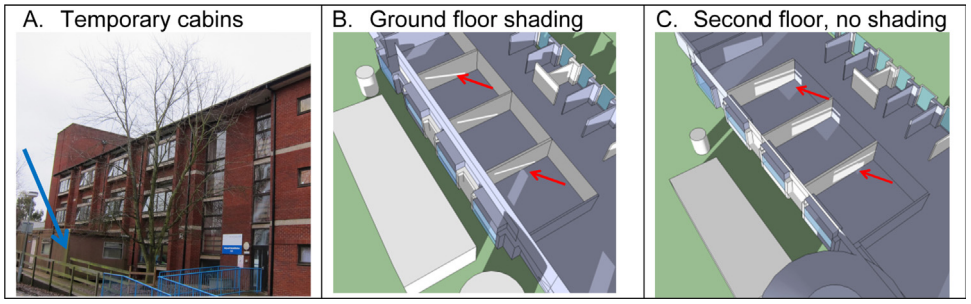

Fig. 5. St Albans, masonry slab building with temporary cabins (blue arrow) adjacent to wards SMs-W1$_{gf}$ and SMs-W2$_{gf}$ (A). SketchUp shadow plots for 19:00, 21st July, indicate (red arrows) the different areas of direct sunlight entering through the windows on the ground floor (B) and second floor, SMs-W1$_{sf}$ and SMs-W2$_{sf}$, (C). (For interpretation of the references to color in this figure legend, the reader is referred to the web version of this article.)

Table 2
Coefficient values of fitted distribution lag models (DLMs), their associated standard error, and each DLMs coefficient of determination, for five rooms at Bradford Royal Infirmary, generated using data from the summer of 2011.

Coefficient and dimensions	Coefficients in DLM (coefficient's standard error)				
	BMa-E	BMa-W	BNi-W	BMo-E	BMo-W
c °C	1.940 (0.167)	1.426 (0.169)	0.250 (0.067)	0.636 (0.094)	0.960 (0.137)
α_1 °C	0.981 (0.032)	0.871 (0.025)	1.016 (0.023)	1.176 (0.024)	1.007 (0.067)
α_2 °C	−0.119 (0.031)	−0.002 (0.025)	−0.070 (0.022)	−0.226 (0.023)	−0.071 (0.063)
α_3 °C	0.036 (0.008)	0.060 (0.008)	0.038 (0.006)	0.013 (0.005)	0.002 (0.004)
β_0 °C	0.024 (0.003)	0.013 (0.003)	0.005 (0.001)	0.013 (0.002)	0.027 (0.003)
$\nabla\beta_1$ °C	0.046 (0.015)	0.048 (0.013)	0.045 (0.009)	0.037 (0.008)	0.012 (0.008)
γ °C m^2 W^{-1}	0.00006 (0.00006)	0.00008 (0.00007)	0.00003 (0.00006)	0.00009 (0.00003)	0.00040 (0.00004)
$\nabla\gamma_1$ °C m^2 W^{-1}	0.00041 (0.00010)	0.00029 (0.00011)	−0.00025 (0.00006)	0.00007 (0.00005)	−0.00017 (0.00006)
δ °C m^2 W^{-1}	0.00177 (0.00035)	0.00052 (0.00010)	0.00030 (0.00004)	0.00038 (0.00010)	−0.00008 (0.00004)
$\delta_3\nabla_3$ °C m^2 W^{-1}	0.0065 (0.00014)	0.00030 (0.00005)	0.00016 (0.00003)	0.00033 (0.00005)	0.00009 (0.00002)
δ_{23} °C m^2 W^{-1}	0.00104 (0.00017)	0.00020 (0.00009)	0.00001 (0.00003)	0.00043 (0.00007)	0.00025 (0.00004)
δ_{24} °C m^2 W^{-1}	−0.00085 (0.00035)	−0.00034 (0.00010)	−0.00012 (0.00004)	−0.00018 (0.00009)	−0.00008 (0.00004)
R^2	0.8821	0.8729	0.9672	0.9647	0.9757
$\hat{\sigma}_u$	0.5642	0.4850	0.2486	0.2801	0.2136

For coefficients of DLM for St Albans spaces see appendix.

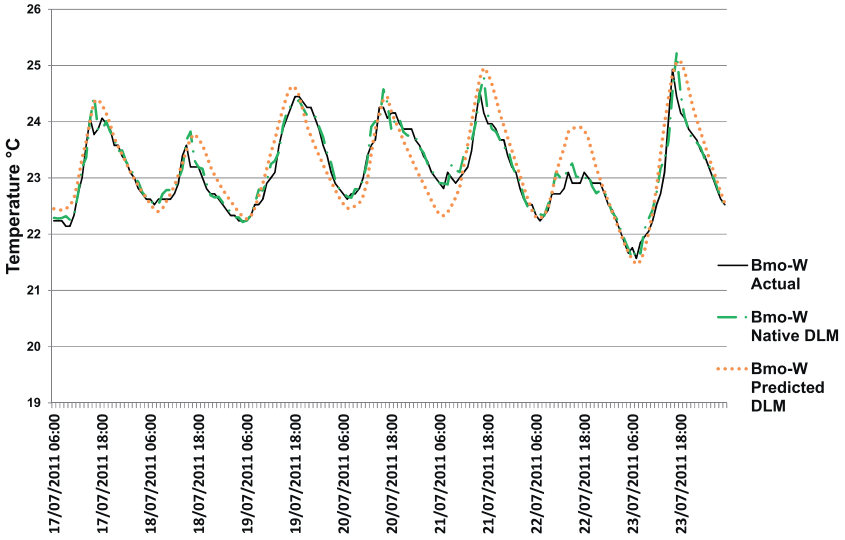

Fig. 6. Comparison of the measured internal temperatures in ward BMo-W, during one week in July 2011 and the temperatures calculated by the native DLM and by the predictive form of the DLM.

(Table 2)[4] the five DLMs explain between 87% and 98% of the variation in room temperature.

For coefficients of DLM for St Albans spaces see appendix.

There is a strong correlation between the recorded internal temperatures and those calculated by the native DLM model using recorded internal temperatures. The agreement obtained for one week in the summer (Pearson correlation 0.99, RMSE 0.22)[5] for one space is illustrated in Fig. 6 (see video files (videos 02–06) in electronic appendix for results over the whole summer for all Bradford spaces tested).

To predict future temperatures in a space, the model will be driven by the exogenous variables as given in a weather file for the period of interest. The previous internal temperatures (at $t-1$, $t-2$ and $t-24$) will though, be the predicted temp resulting from the DLM model, rather than actual measured values. The predictions obtained by the DLM used in this mode, are also plotted in Fig. 6. The temperature trace reproduces reasonably well the measured values but is noticeably smoother. This is because the effects of occupants and other (semi-) random events cannot be captured by the predictive model whereas the native DLM is reset at each time step to the known measured value.

The predictions shown in Fig. 6 were obtained by seeding the DLM with 24 h of actual recorded data from 30th April, before allowing it to continue in predictive mode. However, tests have shown that the DLM can be seeded with a fixed internal temperature at $t-1$, $t-2$ and $t-24$, of say 20 °C, and it will, after 10 days of being driven by the exogenous variables, start to generate good internal temperature predictions.

2.4. Exogenous effects

It is difficult to assess the contributions of each of the exogenous factors on the internal temperature because the values of external temperature are 10–50 times smaller (e.g. 0–25 °C) than the values of solar radiation (0–700 W/m^2). Therefore, an analysis was taken to

[4] R^2 is the square of the Pearson Product Moment Correlation Coefficient and estimates the fraction of the variance in Y that is explained by X.

[5] Pearson Product Moment Correlation Coefficient is a measure of the linear correlation between two variables X and Y giving a value between +1 and -1 inclusive. It is the covariance of the two variables divided by the product of their standard deviation.

Table 3
Calculating the monthly average hourly effect of the exogenous variables on the room temperature.

Contribution of previous internal temperatures	$\frac{\sum_1^j \alpha_1 T_{t-1}+\alpha_2 T_{t-2}+\alpha_3 T_{t-24}}{j}$
Contribution of external temperature	$\frac{\sum_1^j \beta_0 T_{ext_t}+\beta_1 \nabla T_{ext_t}}{j}$
Contribution of global solar radiation	$\frac{\sum_1^j (\gamma_0+\gamma_1) S_{global_t}+\gamma_1 \nabla S_{global_t}}{j}$
Contribution of incident solar radiation	$\frac{\sum_1^j (\delta_0+\delta_3) S_{incident_t}+\delta_3 \nabla_3 S_{incident_t}+\delta_{23} S_{incident_{t-23}}+\delta_{24} S_{incident_{t-24}}}{j}$

j = number of days in the month.

calculate the monthly average hour contribution of each exogenous driver to the DLM of each ward (Table 3).

The resulting hourly contributions averaged for June 2011 (Fig. 7) demonstrate that the most important contributor is the previous room temperatures, with values circa 22 °C, compared to the contribution from the exogenous drivers (external temperature, global solar radiation and incident solar radiation), which each contribute between −0.2 °C and 0.8 °C.

There are clear differences in the contribution of the exogenous variables depending on the building type. Most obviously, the contributions of solar radiation and external temperature to the internal temperature in the Nightingale ward (Fig. 7B) are much lower than for the other wards. This perhaps reflects the heavyweight nature of the Nightingale structure which is known to attenuate the effects of external influences. The results also demonstrate that the incident solar radiation is important in establishing the different diurnal profiles observed in rooms of different orientation (west, Fig. 7A; east, Fig. 7C); this was hypothesised with regard to Fig. 1.

Interestingly, this analysis shows that for BMo-W, Fig. 7D, the contribution of incident solar radiation to internal room temperature after 18:00 h is zero or less. This correlates with the time when the building is shaded of an adjacent building. (A SketchUp shadow cast model showed that the timing of the shading in fact varied through the year: from 17:00 h in June to 14:00 h in December.)

To further investigate DLMs' ability to identify shading effects, a summertime model was developed for wards in the tower building at St Albans. One ward, SMa-E, was orientated to the south east (135°) with a circa 3.2 m overhang located above the window. SketchUp models predicted that this overhang would block incident solar radiation falling on the room façade after 10:00 during

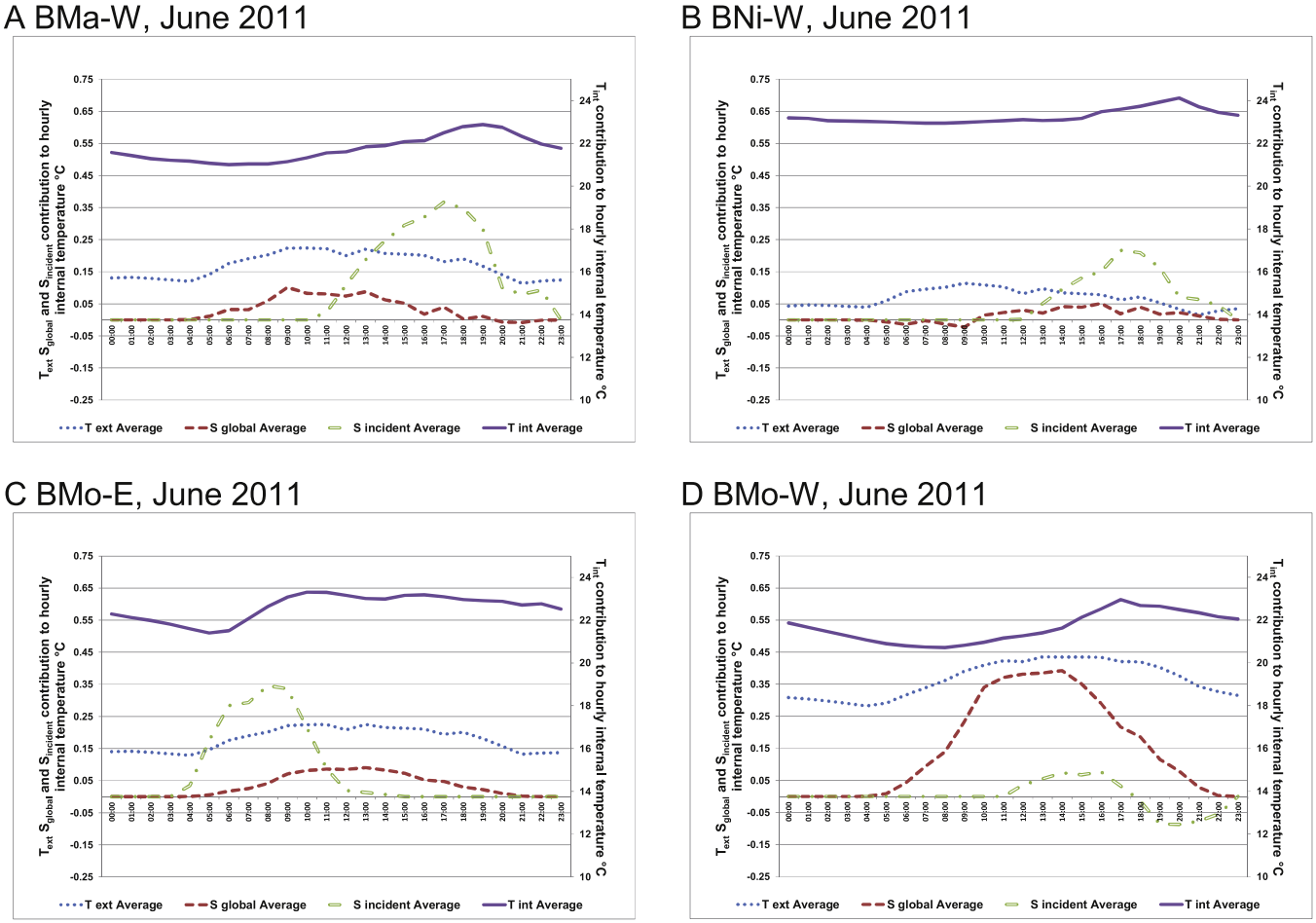

Fig. 7. Monthly average hourly contribution of the exogenous drivers to internal room temperature in June 2011 as indicated by the DLM for four spaces at Bradford Royal Infirmary: exogenous variables, *lh* axis, previous internal temperatures, *rh* axis.

Table 4
Comparison of the correlations between the measured internal temperatures and the temperatures calculated by both the native DLM and the predictive DLM: five wards all at Bradford Royal Infirmary, during the summer of 2011.

	BMa-E		BMa-W		BNi-W		BMo-E		BMo-W	
	RMSE	R^2	RMSE	R^2	RMSE	R^2	RMSE	R^2	RMSE	R^2
Native DLM	0.75	0.82	0.48	0.90	0.24	0.96	0.29	0.97	0.22	0.97
Predictive DLM	1.73	0.31	1.20	0.37	1.07	0.17	1.34	0.35	0.98	0.59

Table 5
Comparison of the measured hours over 25 °C and 28 °C in the summer of 2011 with the predictions of the native and predictive DLMs for five spaces. Entries are number of hours in the summer of 2011 (1st May–30th September) and the percentage of all hours in this period.

	BMa-E		BMa-W		BNi-W		BMo-E		BMo-W	
	25 °C	28 °C	25 °C	28 °C	25 °C	28 °C	25 °C	28 °C	25 °C	28 °C
Measured	427 (11.6%)	13 (0.4%)	474 (12.9%)	12 (0.3%)	82 (2.2%)	0 (0%)	755 (20.6%)	21 (0.6%)	331 (9%)	10 (0.3%)
Native DLM	440 (12%)	44 (1.2%)	482 (13.1%)	14 (0.4%)	88 (2.4%)	0 (0%)	748 (20.4%)	26 (0.7%)	354 (9.6%)	10 (0.3%)
Predictive DLM	638 (17.4%)	185 (5%)	696 (19%)	0 (0%)	65 (1.8%)	0 (0%)	907 (24.7%)	11 (0.3%)	507 (13.8%)	25 (0.7%)

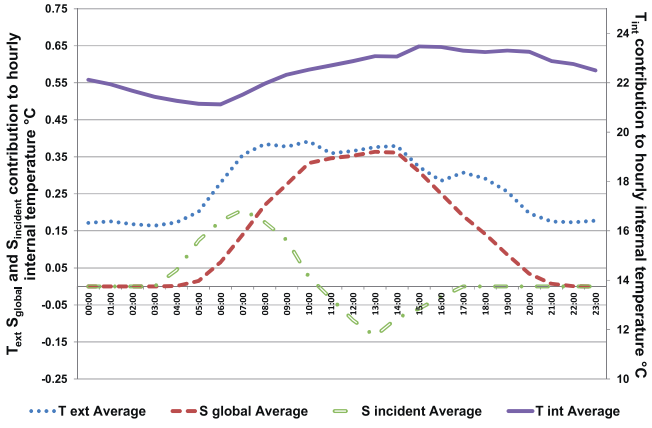

Fig. 8. Monthly average hourly contribution of the exogenous drivers to internal room temperature in June 2011 as indicated by the DLM for a south east facing ward, SMa-E, with a shading overhang: exogenous variables, *lh* axis, previous internal temperatures, *rh* axis.

the summer. Remarkably, this correlates with the time when the exogenous contribution of incident solar radiation in the DML was zero or below (Fig. 8 shows June 2011).

Similar studies also revealed the DLMs' sensitivity to shading (results not shown). For example, the contribution of incident solar radiation was greater in the DLM for SMs-$W2_{sf}$ than in the DLM for SMs-$W1_{sf}$, which correlates with the fact that SMs-$W1_{sf}$ is partially shaded by an adjacent deciduous tree (visible in Fig. 5A).

2.5. Predictive abilities of the models

To understand the performance of the DLMs, the measured internal temperatures for the whole of the summer of 2011 were compared with the calculations of the native DLM and the results of the predictive DML for all five wards (Table 4). This revealed the weaker capability of the predictive model compared to the DLM in its native mode (native DLM: RMSE 0.22–0.75, R^2 0.82–0.97; predictive DLM: RMSE 0.98–1.41, R^2 0.31–0.59).[6] The abilities of the predictive model did though vary from week to week. (In results not shown, the weekly R^2 values for BMo-W varied from 0.18 to 0.90, with a median weekly value of 0.69 and the corresponding RMSE values varied from 0.35 to 1.56, with a median weekly value of 0.59. This indicates that the predictive DLM performs well, in general, for the modelled period, but that sudden internal temperature changes, (perhaps due to occupant effects) cannot be replicated. Comparison of calculations by the native DLM and predictive DLM for all five Bradford spaces over the summer of 2011 can be viewed as video files (Videos 02–06) in the electronic appendix.

Whilst the predictive DLMs do not replicate the exact measured hourly internal temperatures, they do model the underlying trend of the measured temperatures and might be used to predict overheating risk as it is commonly defined. The CIBSE guides for example (CIBSE 2006) indicates that when a building's internal temperature is predicted to exceed 25 °C for more than 5% of occupied hours, or 28 °C for more than 1% of hours, there is an unacceptable overheating risk.

Considering Table 5, the measurements indicate that the number of hours over 25 °C is between 2.2% (of the 3672 h from 1st May to 30th September, 2011) and 20.6%, with the east facing modular ward, BMo-E, producing the highest values. The native DLMs reproduced these figures well, and thus correctly ranked the relative overheating risk of the five wards. In contrast, and ignoring the BNi-W results where the overheating risk was close to zero, the predictive DLMs yielded hours over 25 °C which were between 20% and 53% greater than the measured values. However the wards' overheating risks were correctly ranked. The over prediction is very probably because predictive DLM's are unable to capture effects such as window opening by occupants on the hot days; which suppresses (measured) internal temperatures. Whilst the apparently large differences from the measurements might seem dispiriting it is important to place them in the context of the capabilities of sophisticated dynamic thermal models, which also often predict very different temperatures from those that are measured (see Section 3).

With the exception for BMa-E, the absolute number of hours over 28 °C produced by the predictive DLMs are also close to the measured values (Table 5). Investigation revealed that the temperature sensor in BMa-E was actually exposed to direct sunlight at 9:00 am each morning and so recording values well above the real average space temperature. The consequence is that the DLM coefficients will over emphasise the contribution of the exogenous driver for incident solar radiation leading to higher than measured temperatures being predicted. The data for BMa-E is therefore not used in further DLM evaluations.

Most encouragingly, the predictive DLMs correctly identified the spaces that would be classed as having an unacceptable overheating risk, as judged by either the 5% over 25 °C or 1% over 28 °C criterion. The potential of predictive DLMs for indicating spaces at risk of overheating is explored later in this paper.

[6] Root Mean Square Error (RMSE) measures the mean difference between values predicted by a model and those actually observed.

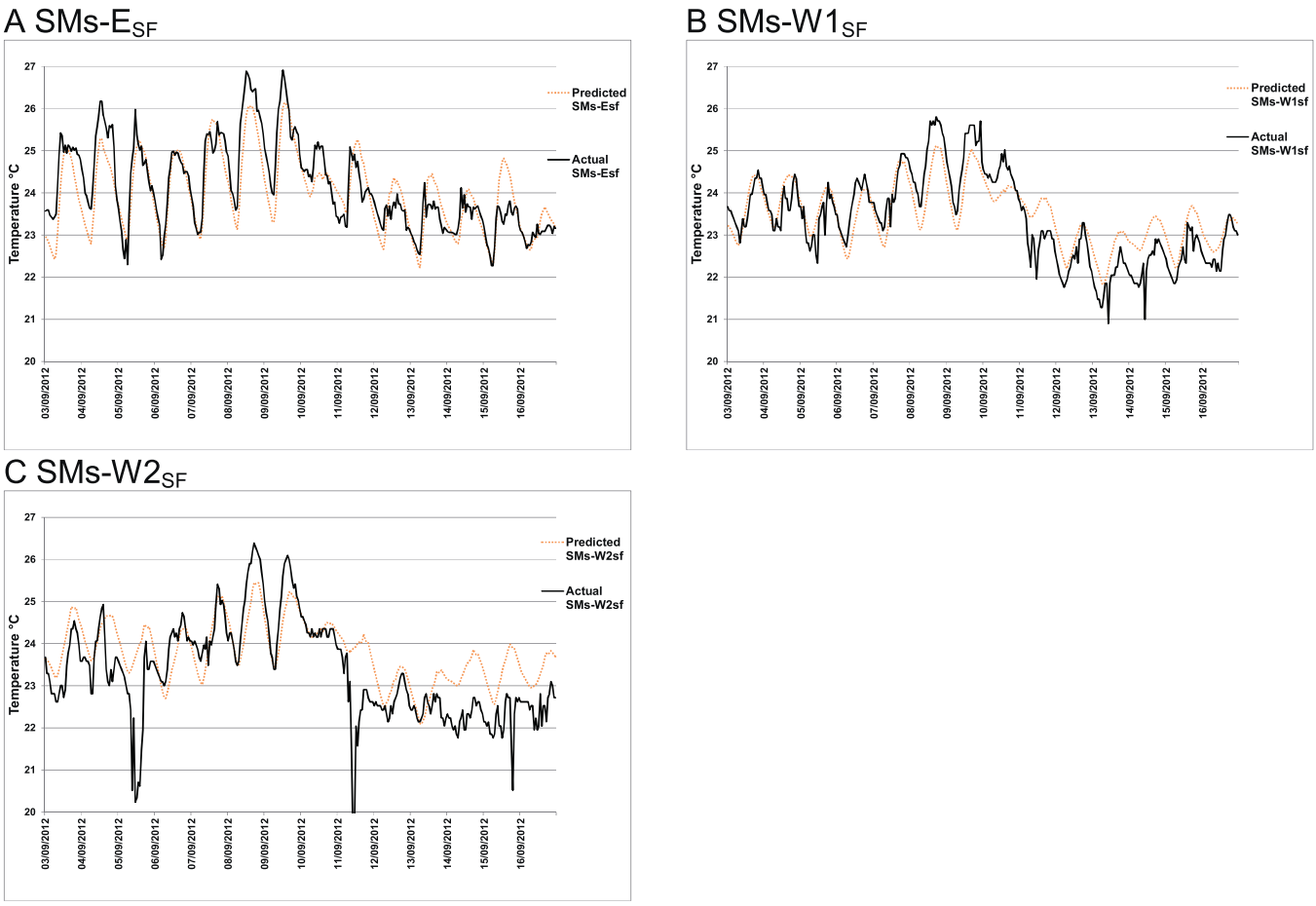

Fig. 9. Comparison of measured internal temperatures and values from predictive DLM for a two week period in September 2012.

Considering the actual performance of buildings for a moment, it is evident that the risk of overheating is much less in the thermally heavyweight Nightingale wards than in the others. The severe overheating risk, as measured by hours over 25 °C, in the lightweight modular wards is evident, with the east-facing wards being at higher risk than the west-facing wards.

2.6. Validation

The DLMs for nine spaces listed in Table 1 were developed using data for the summer of 2011. Clearly, to be of value, predictive DLMs must be able to forecast accurately the internal temperatures that will occur under a different set of summer conditions.

To test the DLMs' forecasting ability, the exogenous variables recorded for the summer of 2012 i.e. local weather data, at St Albans, were fed into the DLMs of three wards, SMs-E_{sf}; SMs-$W1_{sf}$ (which had partial tree shading) and SMs-$W2_{sf}$, and the predicted internal temperatures compared with those actually measured. (2012 room data was only available for the St Albans site.)

The three predictive DLMs were seeded on 1st May, with 24 h of recorded data, but the results indicated that the model only approached the measured data from 1st June onwards. This appeared to be because the wards were under the influence of the heating system until late May (results not shown), whereas the model, of course, was developed using measurements when there was no heating. For the period from June to Spetember 2012, the predictive DLM's results followed the measurements reasonably well, RMSE from 0.61 to 0.87; and R^2 between 0.55 and 0.76 (full summer results are available in the video appendix, videos 07–09).

Notable discrepancies did occur though when there were sudden erratic changes in the measured values (Fig. 9). For example on September 11th, following two hot days on the 8th and 9th, the predicted values were well above the measured values, especially for the unshaded second floor ward (SMa-$W2_{sf}$). It is possible that the hot spell, resulted in windows being left open for a long period of time, or, indeed, that portable air-conditioning was used.

For the two spaces that did not experience erratic temperature changes, the number of hours over 25 °C produced by the predictive DLM were similar to the number measured (Tables 6 and 7).

The relative overheating risk of the spaces, as indicated by the number of hours over 25 °C, is correctly predicted by the DLMs; with SMs-E_{sf} being the warmest ward and SMs-$W1_{sf}$, the partially

Table 6
Comparison of the measured hours over 25 °C and 28 °C in the summer of 2012 with the predictions of the DLM for three spaces.

	SMs-E_{sf}		SMs-$W1_{sf}$		SMs-$W2_{sf}$	
	25 °C	28 °C	25 °C	28 °C	25 °C	28 °C
Measured	483 (16.5%)	20 (0.7%)	294 (10%)	0 (0%)	365 (12.5%)	16 (0.5%)
Predictive DLM	452 (15.4%)	0 (%)	255 (8.7%)	0 (0%)	405 (13.8%)	0 (0%)

Table 7
Root mean square errors and R^2 values of the predictions of the DLM for three spaces in the summer of 2012 compared to the measured temperatures. The results demonstrate good correlations with predicted data.

	SMs-E_{sf}		SMs-$W1_{sf}$		SMs-$W2_{sf}$	
	RMSE	R^2	RMSE	R^2	RMSE	R^2
Predictive DLM	0.78	0.69	0.61	0.76	0.74	0.55

shaded ward, the coolest. Both the measurements and the predictive models indicate that all wards exceed the CIBSE 5%/25 °C threshold but none exceed the 1%/28 °C threshold.

2.7. Forecasting performance and heat waves

Models of spaces are of course most useful when thermal performance under conditions for which performance has not been measured is reliably predicted. The UK NHS is especially interested in the internal temperatures likely to occur in spaces during heat waves; as hospitals need to provide a safe haven during such events. Therefore, weather data collected at London Heathrow Airport, during the summer of 2006, when Europe experienced a severe heat wave, was used to drive the predictive DLMs. The week from 16th to 23rd July 2006 was especially warm, with five consecutive days having a daily maximum temperature over 31 °C with an absolute peak of 35 °C; a severe heat wave is announced in the UK when two or more consecutive days exceed 31 °C [10].

The predictions obtained for four wards at Bradford and for four at St Albans indicate that for almost the entire week of the heat wave the internal temperatures in all the buildings would, without occupant intervention, have exceeded 26 °C (Fig. 10). This, according to the NHS heat wave guidance, is the temperature above which vulnerable people are physiologically unable to cool themselves efficiently, and so hospitals are encouraged to ensure cool areas are created that do not exceed 26 °C [10,12]. The modular wards at Bradford Royal Infirmary (BMo-W and BMo-E) were much the hottest, reaching close to 34 °C, and the Nightingale wards (BNi-W) the coolest, reaching only 29 °C (Fig. 10A). The wards in the tower buildings at Bradford (BMa-W) and St Albans (SMa-E) show similar internal temperature profiles, reaching c31 °C. The traditional masonry construction of three wards at St Albans (SMs-E_{SF}, SMs-$W1_{SF}$ and SMs-$W2_{SF}$) seems, like the massive stone construction of the Nightingale wards, to provide resilience to overheating, they reached a peak temperature of c29 °C (Fig. 10B).

To investigate further, the occurrences of temperatures over thresholds of significance (25 °C, 28 °C and 26 °C) were investigated for the severely hot week as well as for the entire summer of 2006 (June–September) using the Heathrow weather data as exogenous driver. Also examined were the thermal comfort conditions as measured by the adaptive criteria of the BSEN15251 standard [28].

The standard enables the 'ideal' internal comfort temperature to increase as the running mean of the external temperature increases. This reflects the adaptation of individuals to warmer ambient conditions (such as wearing fewer or lighter cloths, taking cool drinks or being less active). Four comfort bands, of increasing width around the ideal are defined, Cat.I, a high level of expectation (±2 °C), Cat.II, normal level of expectation (±3 °C), Cat.III, an acceptable moderate level of expectation (±4 °C) and Cat.IV, values outside Cat. IV, which should be accepted for only a limited part of a year. The second author of this paper has argued [14,16] that the BSEN15251 standard is far more appropriate for assessing hospital temperatures than the existing standards, and this is reflected in the recent CIBSE Technical Memorandum TM52 [28,29].

The standard offers several ways of determining the overall comfort category of a space. One way, that is used here, is to simply count the predicted number of hours for which the indoor temperature falls between the threshold temperatures for each category.

No matter whether the fixed overheating risk criteria or the adaptive thresholds are used, the predictions rank the buildings in virtually the same order (Table 8). The coolest wards were in the Bradford Nightingale building (BNi-W) and those in the St Albans masonry building (SMs-E_{sf}, SMs-$W1_{sf}$ and SMs-$W2_{sf}$), with the shaded ward being particularly cool (SMa-$W1_{sf}$). In these spaces, save for a single hour, thermal comfort remained within the Cat.II envelope for the whole summer; 26 °C was only exceed for c20% of the time. These results confirm the findings of earlier research which indicated the remarkable resilience of Nightingale wards to elevated ambient temperatures [14].

The tower buildings at Bradford and St. Albans performed better than the modular wards but worse than the masonry buildings. During the summer, temperatures in these wards (BMa-W and SMa-E) exceeded the Cat.II thresholds c14% of the time and exceeded 26 °C for 30–50% of the time; and the lower value for ward SMa-E is consistent with the presence of the overhang that causes solar shading (see Fig. 8).

The modular building is by far the hottest, with the east-facing ward, as noted above being dangerously hot (BMo-E). Temperatures fell outside the Cat.II threshold for almost 40% of the summer, that is, for 9 h each day on average. The 26 °C danger threshold was exceeded for 78% of the entire summer. The west facing modular ward (BMo-W) performed better, exceeding 26 °C for 47% of the summer; the Bradford tower (BMa-E) performed in a similar way. These results suggest that these spaces will become a danger to patients, staff and visitors during prolonged periods of hot weather unless remedial action is taken.

Such remedial action to maintain habitability, e.g. by facilities managers, nursing staff, or others, would need to be far more substantial in the modular building, or the tower buildings, than in the Nightingale or masonry buildings. For example, whilst night time ventilation, and perhaps the use of fans could render the heavyweight buildings habitable (see [16]), portable air-conditioners might be needed in the modular wards – this is indeed what happened in hot June 2013, which was much less severe than July 2006.

Also of interest in these results is the apparent conflict between the BSEN15251 comfort indication (Cat.II) and the DoH measure of physiological risk (26 °C). This is, of course, because the BSEN15251 envelope encompasses 26 °C when ambient temperatures are high. Such matters require further investigation. In particular, whether the BSEN15251 criteria are appropriate for all wards (perhaps not for those with thermally vulnerable patients) or, conversely, whether the DoH criterion is unnecessarily cautious for some wards (those with relatively healthy patients).

3. Discussion

It is worthwhile reflecting on the strengths and weaknesses of empirically-derived distributed lag models (DLMs) and to compare this approach with the more usual strategy of using dynamic thermal models. The internal temperatures likely to be experienced in hospital wards of different type during heat waves are then discussed; again comparing the messages from the DLMs with

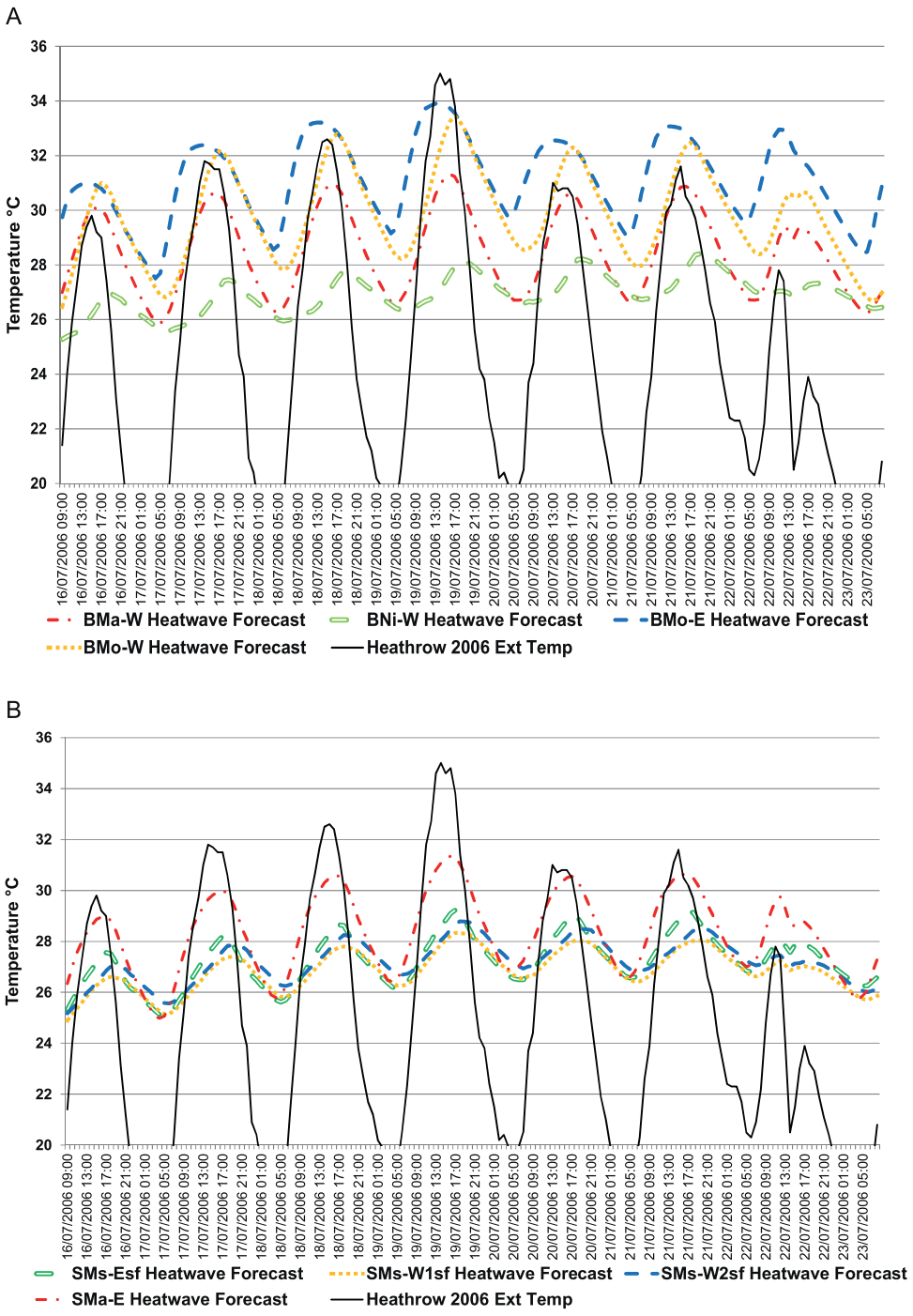

Fig. 10. Internal space temperatures predicted by the DLMs of eight spaces during the severe heat wave of 2006 (Heathrow weather data for 16–22nd July): (A) predicted internal temperatures in four wards at Bradford Royal Infirmary; and (B) predicted internal temperatures in four wards at St Albans Hospital. (Predicted temperatures for the whole perion from June to September 2006 can be found in electronic appendix.)

those from previous dynamic thermal modelling studies. Finally, the potential of temperature monitoring, and the automatic generation of DLMs, is discussed as a basis for predictive control of internal environments and the provision of overheating risk warnings.

In the work presented here, the native DLMs predicted temperatures in the next hour using 12 parameters relating to: past internal temperatures (3); exogenous 'drivers', external temperature (2), global radiation (2) and calculated incident solar radiation (4); and a constant. The models' parameters, and the values of the coefficients, were generated by the eViews software. No attempt was made to search for particular formulations or to further refine the parameters in the model or their coefficients. This approach to generating DLMs is therefore tractable by non-expert statisticians. The form of the models, and the relatively small contribution of some variables does, though, suggest, that simpler formulations may exist. Deletion of some parameters may be possible with little detriment to the models' accuracy.

The derived, space-specific, DLMs inherently account for: known thermally-important features, insulation levels, window areas, etc.; difficult-to-measure parameters like mechanical ventilation rates and infiltration rates, and the inevitable but

Table 8
Number of hours for which internal temperatures predicted by DLMs exceed particular benchmark temperatures, or falls within the comfort categories defined in BSEN15251 during: (A) the hot summer of 2006; and (B) the severe heat wave week of 16–22 July 2006.

		Bradford RI				St Albans Hospital			
		BM5-MB201 Tower (240° N)	BW8-TB02 Nightingale (270° N)	BW29-SB101 Modular (90° N)	BW29-MB101 Modular (270° N)	SR3-SB101 Masonry (135° N)	SR3-MB102 Masonry (315° N)	SR3-MB201 Masonry (315° N)	SM5-MB102 Tower (315° N)
June to September 2006	>25	2222 (75.9%)	1149 (39.2%)	2760 (94.3%)	1968 (67.2%)	1179 (40.3%)	964 (32.9%)	1262 (43.1%)	1299 (44.4%)
	>26	1488 (50.8%)	529 (18.1%)	2283 (78%)	1378 (47.1%)	642 (21.9%)	469 (16%)	609 (20.8%)	863 (29.5%)
	>28	490 (16.7%)	14 (0.5%)	1211 (41.4%)	618 (21.1%)	89 (3%)	13 (0.4%)	57 (1.9%)	280 (9.6%)
	I	2146 (73.3%)	2925 (99.9%)	1138 (38.9%)	2080 (71%)	2822 (96.4%)	2912 (99.5%)	2857 (97.6%)	2317 (79.1%)
	II	355 (12.1%)	3 (0.1%)	650 (22.2%)	342 (11.7%)	105 (3.6%)	16 (0.5%)	71 (2.4%)	209 (7.1%)
	III	226 (7.7%)	0 (0%)	468 (16%)	222 (7.6%)	1 (0%)	0 (0%)	0 (0%)	341 (11.6%)
	IV	201 (6.9%)	0 (0%)	672 (23%)	284 (9.7%)	0 (0%)	0 (0%)	0 (0%)	61 (2.1%)
Severe Heatwave week 16–22 July 2006	>25	168 (100%)	168 (100%)	168 (100%)	168 (100%)	162 (96.4%)	160 (95.2%)	165 (98.2%)	160 (95.2%)
	>26	161 (95.8%)	141 (83.9%)	168 (100%)	164 (97.6%)	143 (85.1%)	140 (83.3%)	148 (88.1%)	151 (89.9%)
	>28	96 (57.1%)	14 (8.3%)	158 (94%)	143 (85.1%)	41 (24.4%)	13 (7.7%)	33 (19.6%)	93 (55.4%)
	I	82 (48.8%)	165 (98.2%)	4 (2.4%)	30 (17.9%)	132 (78.6%)	158 (94%)	144 (85.7%)	83 (49.4%)
	II	25 (14.9%)	3 (1.8%)	20 (11.9%)	42 (25%)	35 (20.8%)	10 (6%)	24 (14.3%)	26 (15.5%)
	III	29 (17.3%)	0 (0%)	29 (17.3%)	29 (17.3%)	1 (0.6%)	0 (0%)	0 (0%)	38 (22.6%)
	IV	32 (19%)	0 (0%)	115 (68.5%)	67 (39.9%)	0 (0%)	0 (0%)	0 (0%)	21 (12.5%)

CatII means additional hours between CatI and CatII thresholds, etc.
Values in brackets are the percentage of total hours, which is 168 h (16–22 July) and 3672 h (June–September).

unquantifiable thermal effects, such as heat gain from hot water pipes (important in hospitals) and heat bridges. All these must be explicitly accounted for in dynamic thermal models, so often the input values are just assumed. This difficulty is entirely avoided with DLMs.

Predictive DLMs, which do not include the measured temperature at previous time points, reproduce internal temperatures much less reliably than native DLMs (which do). They cannot account for sudden eccentric changes in internal temperatures as a result of occupant behaviour (and other random events), although neither can calibrated dynamic thermal models (see for example the calibration graphs in [15,16]). The predictive DLMs do though capture the underlying effect of such behaviours on internal temperature. This is important, especially when occupant effects are systematic, opening of windows at a certain time each day or when temperatures exceed a certain level, or the closing of blinds (shading) in response to time of day (dusk for example) or weather conditions.

The limitation, of the DLMs is, of course, that they can only predict the effects of changes to the exogenous drivers (and past internal temperatures). Recalculation of the empirical coefficients would be necessary to test the effects of changes to the building or its HVAC systems. In contrast, such changes can readily be examined by dynamic thermal models, which have been used to explore the added resilience to hot weather conferred by energy-efficient remodelling of the buildings at the Bradford [14], Addenbrooke's, Cambridge [16,17] and Glenfield, Leicester hospitals [15].

The predictive DLM for any space is built from simple-to-make temperature measurements and predictions of future temperatures are made for the same locations as the measurements. The measurements should ideally be made under conditions similar to those for which predictions are to be made (so that ventilation and occupant behaviours are reasonably well characterised). This is, of course, difficult when extreme weather events of a magnitude as yet not experienced, are being studied. This problem is also encountered in the calibration of dynamic thermal models.

The results from the predictive DLMs conferred credibility. They reflected the expected impact on internal temperatures of room orientation and site and facade shading. Indeed, the DLMs revealed the very existence of the shading objects to the researchers; they would very likely have been overlooked, and their substantial impact missed, had dynamic thermal modelling been used. The DLMs also revealed, the similarity in the predicted incidence of elevated temperatures in buildings with similar construction and ventilation strategy (when they were exposed to the same weather); even when the DLMs were developed from data gathered at a different sites: the mixed-mode, concrete-frame tower building in St Albans (SMa) performed similarly to the tower at Bradford (BMa). The validation study indicated that the predictive DLMs (generated from 2011 summertime measurements) could reliably to predict the internal temperatures measured under different weather conditions; those during the summer of 2012.

Concerning the performance of the hospital wards, it is evident from the measurements and the DLMs, that thermal mass confers resilience to elevated external temperatures and that the more thermally massive the building the more resilient it was to hot external conditions. (Although other thermally influential features also change as the thermal mass changes, ceiling heights, window-to-floor ratios, infiltration rates, etc.) Thermal mass, and associated other thermal effects, conferred resilience irrespective of whether the building was ventilated entirely naturally (by window opening) or by a mix of natural and mechanical ventilation.

The predictive DLMs showed that the wards with little thermal mass would very probably become dangerously hot in heat waves such as those experienced in 2006. During the hottest week of 2006,

the predictive DLMs indicted that the Bradford modular building would, without intervention, exceed 28 °C for 20 (west-facing) to 22 (east-facing) hours per day on average. This is dangerously hot, far above that recommended. This is particularly worrying as UK hospitals are expected to provide a safe haven for those most vulnerable to heat waves. Intervention, such as permanent external shading, would seem prudent, and even so, temporary air-conditioning may be needed during very hot weather. It is fortunate that Bradford is less likely to suffer hot weather events than areas further south and east in the UK.

The DLM results are in line with those previously reported, which were obtained from dynamic thermal models; most notably the thermal resilience of the Nightingale wards in Bradford [14] compared to a concrete-frame tower in Cambridge [16,17].

More generally, lightweight modular buildings, without any external shading, like those at Bradford, are especially dangerous during heat waves; from a heat wave perspective, they would appear to be an unwise built form, especially for hospital wards. Perhaps, advice to hospital managers which is based on a model of their actual building's performance (e.g. a DLM), may well be acted on more readily than information based on other, abstract, model types.

Finally, it is worth thinking about the advice and space management possibilities of DLMs. Strategic advice to building owners and operators might, for example, concern the likely performance of an existing new building in weather conditions as yet not experienced (e.g. the likely impact of a heat wave). The results might act as a spur to retrofit in order to stave off an undesirable future event. This work suggests, for example, that the installation of external shading on the Bradford modular buildings would be a good idea. Undertaken more widely, temperature monitoring, and the creation of DLMs, might be used to ascertain the overheating risk of whole building stocks. Internal temperatures could be monitored over a summer period (the optimum length of period has yet to be established by the authors) and used to generate DLMs which could then be employed with various weather scenarios to predict performance. The exceedance of standard values (e.g. hours above 26 °C or BSEN15251 categories) could then be used to assign an overheating risk value to the monitored space. Indeed, historical room temperature data may already be available for numerous spaces, as recorded by building management systems for example.

The DLM approach also has potential for *managing* space temperatures in existing naturally ventilated and mixed-mode buildings. In particular, it may be possible to install air temperature sensors linked to an occupant warning or automatic controller. (Although temperature sensors are small and low cost, they must be sited carefully to avoid spurious data; some in this study were seen to be in direct sunlight at certain times.) The created DLMs could provide near term predictions of internal temperature on the basis of weather forecasts (simply waiting for heat wave warnings may be inadequate for the least resilient buildings). The predictions could be the basis of warnings to building managers or nursing staff, who might, for example, open windows for night cooling, closing solar shading devices, or install portable fans. Alternatively, the models might be used to operate actuators on windows, shading devices or ventilation openings to automatically guard occupants form impending weather events.

4. Conclusions

This paper presents a novel methodology for forecasting hourly internal temperatures in buildings without the need for complicated and time consuming computerised dynamic thermal modelling. By applying time series analysis to monitored internal temperature data, distributed lag models (DLM) were developed. The native DLMs predicted temperatures an hour ahead based on past internal temperatures and external temperature and solar radiation measurements, predictive DLMs used only the external drivers to make future predictions of internal temperatures.

Using standard statistical analysis software, DLMs were easily created from temperature measurements made during the summer of 2011 in 97 naturally ventilated and mixed-mode wards, on hospital four sites, in the UK. This paper presents results for 11 wards on two sites, Bradford, in the north of England, and St Albans in the south east.

The DLMs capture the inherent known and unknown thermophysical and human influences on space temperatures. They revealed the substantial impact that orientation and site shading has on internal temperatures and actually revealed shading effects previously unnoticed by the researchers (trees and temporary buildings).

Temperatures measured in the same wards during the summer of 2012 were used to validate the results from the predictive DLMs by driving them with the measured 2012 weather data. The results were encouraging, with the differences from the measurements being due to unknown and unpredictable eccentric events, such as occupants opening windows; such events are impossible to capture reliably with any long-term predictive tool. DLMs may be just as reliable at predicting responses to external weather events as calibrated dynamic thermal models; but they are much easier and quicker to create. This is an area worthy of further investigation.

The measurements made during the summer of 2011, and the predictions of the DLMs, showed that east facing wards tended to heat up earlier in the day and so record more hours over any chosen threshold temperature than west facing wards. In general, the wards in the thermally light-weight, mixed-mode, modular building at Bradford and those in the concrete-framed, mixed-mode tower building, were much warmer, and uncomfortably so, than the naturally ventilated, thermally massive Nightingale ward.

Hospital wards' performance during a severe heat wave was assessed by feeding the predictive DLMs with the weather data recorded at Heathrow, London during the European heat wave of 2006. The predicted internal temperatures were assessed using the CIBSE steady state criteria (hours over 25 °C and 28 °C) and the BSEN15251 adaptive criteria. Both types of assessment ranked the wards' resilience to heat waves in virtually the same order. The Nightingale ward was the most resilient with, during the hottest week (16–22 July 2006), just 2 h per day, on average, over 28 °C. The low-rise masonry building at St Albans was also reasonable resilient, whereas wards in the concrete-frame towers at St Albans and Bradford were much hotter; 28 °C was exceeded for more than 12 h a day on average.

The modular wards were dangerously hot. During the hot week of the 2006 heat wave the DLMs predicted 20 or more hours per day over 28 °C; temperatures exceeded the UK Department of Health safe threshold, of 26 °C, for the entire week. It is evident that mixed-mode, unshaded and thermally lightweight construction, such as that at Bradford, could be a danger to occupant health during a severe heat wave. Substantial intervention, such as the installation of temporary air-conditioning, would be needed to render such buildings habitable. It would seem particularly unwise to adopt such a built-form for hospital wards; they are likely to harbour thermally vulnerable patients, particularly so during a heat wave, when hospitals might be expected to provide a safe haven.

4.1. Further work

Internal temperature can be considered as the phenotype of a space, the observable result of multifactorial static characteristics

affected by numerous transient exogenous influences. The static characteristics may be considered equivalent to a genotype and include space volume, construction materials, orientation of the space with respect to north. Environmental conditions describe the transient exogenous influences such as solar radiation, external temperature, internal heat gains etc. Such that, as in biology, phenotype = genotype + environment. Thus the internal temperature in a building space might be summarised as:

$$\text{phenotype} = \text{ktiriotype} + \text{environment}.$$

The statistical models developed in this study concern only the phenotype (i.e. the internal temperature) and the contribution of some environmental factors, though it is likely that the external factors of solar radiation and external temperature are the principal environmental effects during the summer modelling period. One might assume that the coefficients calculated for each of these exogenous drivers relate in some way to the ktiriotype of an individual space (i.e. the building make-up, equivalent to a genotype), where the ktiriotype is composed of multifactorial contributors (e.g. construction materials, patterns of occupancy, internal heat gains) the significance of these factors on the kteriotype could be further investigated. For example what effect do changes in glazing area have on the coefficients associated with solar radiation? There is not a direct link to the statistical model coefficients and the space ktirotype, these values are unique and specific to individual spaces and thus a universal statistical model that can be used to predict a space phenotype using weather data, without first generating coefficients using hourly internal temperatures recorded over a period of time is unlikely to be possible.

In order to further understand the relationship of the ktiriotype to space phenotype, experimentation could draw on the principle of genetic knockout experiments where the impact of a single gene on a phenotype is investigated [30]. In a similar manner, an aspect of the ktiriotype of a simple structure can be altered (for example changing the glazing size in a test cell, either computational or physical) and the effect on the phenotype (internal temperature) and the magnitude of the distribution lag model coefficients measured.

Acknowledgements

The data used in this paper was collected as part of the UK Engineering and Physical Sciences Research Council (EPSRC) project, DeDeRHECC: '*Design and Delivery of Robust Hospital Environments in a Changing Climate*' (EP/G061327/1), which was funded through the Adaptation and Resilience to a Changing Climate programme. The project was collaboration between Cambridge, Loughborough and Leeds Universities and the Open University. The data collection was made possible by the kind cooperation of the Bradford Teaching Hospitals NHS Foundation Trust and the West Hertfordshire NHS Trust.

Thanks must be extended to a number of people who provided useful discussion and information during the preparation of this paper. Dr David Allinson for useful insight into utilising diurnal profiling as a means to visualise the vast data sets and Kevin Gori of the European Molecular Biology Laboratory who guided our interest into utilising time series analysis on the data sets. Louis Fifield of Loughborough University was responsible for much of the internal temperature data collection and Dr Matthew Eames of Exeter University kindly provided the 2006 Heathrow weather data for use with our forecasting studies.

Appendix A. Supplementary data

Supplementary data associated with this article can be found, in the online version, at http://dx.doi.org/10.1016/j.enbuild.2014.09.053.

References

[1] R. Bustinza, G. Lebel, P. Gosselin, D. Bélanger, F. Chebana, Health impacts of the July 2010 heat wave in Québec, Canada, BMC Public Health 13 (2013) 56, http://dx.doi.org/10.1186/1471-2458-13-56.
[2] X.Y. Wang, A.G. Barnett, W. Yu, G. FitzGerald, V. Tippett, P. Aitken, et al., The impact of heatwaves on mortality and emergency hospital admissions from non-external causes in Brisbane, Australia, Occupational and Environmental Medicine 69 (2012) 163–169, http://dx.doi.org/10.1136/oem.2010.062141.
[3] T. Kosatsky, The 2003 European heat waves, Eurosurveillance 10 (2005) 148–149.
[4] J. Rocklöv, K. Ebi, B. Forsberg, Mortality related to temperature and persistent extreme temperatures: a study of cause-specific and age-stratified mortality, Occupational and Environmental Medicine 68 (2011) 531–536, http://dx.doi.org/10.1136/oem.2010.058818.
[5] C. Wang, R. Chen, X. Kuang, X. Duan, H. Kan, Temperature and daily mortality in Suzhou, China: a time series analysis, Science of the Total Environment 466–467 (2014) 985–990, http://dx.doi.org/10.1016/j.scitotenv.2013.08.011.
[6] C.B. Field, V. Barros, T.F. Stocker, D. Qin, D.J. Dokken, K.L. Ebi, et al. (Eds.), Managing the Risks of Extreme Events and Disasters to Advance Climate Change Adaptation. A Special Report of Working Groups I and II of the Intergovernmental Panel on Climate Change, Cambridge University Press, Cambridge, UK, and New York, NY, USA, Cambridge, 2012, http://dx.doi.org/10.1017/CBO9781139177245.
[7] B. Orlowsky, S.I. Seneviratne, Global changes in extreme events: regional and seasonal dimension, Climatic Change 110 (2011) 669–696, http://dx.doi.org/10.1007/s10584-011-0122-9.
[8] L.V. Alexander, X. Zhang, T.C. Peterson, J. Caesar, B.A. Gleason, M.G. Klein Tank, et al., Global observed changes in daily climate extremes of temperature and precipitation, Journal of Geophysical Research 111 (2006) D05109, http://dx.doi.org/10.1029/2005JD006290.
[9] R.T. Clark, J.M. Murphy, S.J. Brown, Do global warming targets limit heatwave risk? Geophysical Research Letters 37 (2010), http://dx.doi.org/10.1029/2010GL043898.
[10] Department of Health, Heatwave – Protecting Health and Reducing Harm from Severe Heat and Heatwaves, 2012.
[11] R.S. Kovats, S. Hajat, P. Wilkinson, Contrasting patterns of mortality and hospital admissions during hot weather and heat waves in Greater London, UK, Occupational and Environmental Medicine 61 (2004) 893–898, http://dx.doi.org/10.1136/oem.2003.012047.
[12] C. Carmichael, G. Bickler, S. Kovats, D. Pencheon, V. Murray, C. West, et al., Overheating and hospitals – what do we know? Journal of Hospital Administration 2 (2012) 1–7, http://dx.doi.org/10.5430/jha.v2n1p1.
[13] J. Kravchenko, A.P. Abernethy, M. Fawzy, H.K. Lyerly, Minimization of heatwave morbidity and mortality, American Journal of Preventive Medicine 44 (2013) 274–282, http://dx.doi.org/10.1016/j.amepre.2012.11.015.
[14] K. Lomas, R. Giridharan, C.a. Short, Fair, resilience of "Nightingale" hospital wards in a changing climate, Building Services Engineering Research and Technology 33 (2012) 81–103, http://dx.doi.org/10.1177/0143624411432012.
[15] R. Giridharan, K.J. Lomas, C.a. Short, a.J. Fair, Performance of hospital spaces in summer: a case study of a "Nucleus"-type hospital in the UK Midlands, Energy and Buildings 66 (2013) 315–328, http://dx.doi.org/10.1016/j.enbuild.2013.07.001.
[16] K.J. Lomas, R. Giridharan, Thermal comfort standards, measured internal temperatures and thermal resilience to climate change of free-running buildings: a case-study of hospital wards, Building and Environment 55 (2012) 57–72, http://dx.doi.org/10.1016/j.buildenv.2011.12.006.
[17] C.A. Short, K.J. Lomas, R. Giridharan, A.J. Fair, Building resilience to overheating into 1960s UK hospital buildings within the constraint of the national carbon reduction target: adaptive strategies, Building and Environment 55 (2012) 73–95, http://dx.doi.org/10.1016/j.buildenv.2012.02.031.
[18] G. Tsilingiridis, Three-year measurements of ambient and indoor air temperatures in Solar Village-3, Athens, Greece 28 (1998) 127–136.
[19] S. Danov, J. Carbonell, J. Cipriano, J. Martí-Herrero, Approaches to evaluate building energy performance from daily consumption data considering dynamic and solar gain effects, Energy and Buildings 57 (2013) 110–118, http://dx.doi.org/10.1016/j.enbuild.2012.10.050.
[20] M.J. Brook, B.A. Finney, Generation of bivariate solar radiation and temperature time series, Solar Energy 39 (1987) 533–540.
[21] P.J. Schluter, P.M. Macey, R.P. Ford, The relationship between inside and outside ambient temperatures in Christchurch, New Zealand, Paediatric and Perinatal Epidemiology 14 (2000) 275–282.
[22] M.J. Ren, J.A. Wright, Adaptive diurnal prediction of ambient dry-bulb temperature and solar radiation, HVAC&R Research 8 (2002) 383–402.
[23] C. Ghiaus, Experimental estimation of building energy performance by robust regression, Energy and Buildings 38 (2006) 582–587, http://dx.doi.org/10.1016/j.enbuild.2005.08.014.

[24] T.C. Mills, Skinning a cat: alternative models of representing temperature trends, Climatic Change 101 (2010) 415–426, http://dx.doi.org/10.1007/s10584-010-9801-1.
[25] C.A. Short, C.J. Noakes, C.a. Gilkeson, A. Fair, Functional recovery of a resilient hospital type, Building Research and Information 42 (2014) 657–684, http://dx.doi.org/10.1080/09613218.2014.926605.
[26] D.F. Hendry, A. Pagan, J.D. Sargan, Dynamic specification, Chapter 18 of Handbook of Econometrics, vol. II, Amsterdam, 1984.
[27] EViews, 2013, http://www.eviews.com/home.html
[28] British Standard, Indoor environmental input parameters for design and assessment of energy performance of buildings addressing indoor air quality, thermal environment, lighting and acoustics, BS EN 15251.3, 2007.
[29] CIBSE, TM52 the limits of thermal comfort: avoiding overheating in European buildings the limits of thermal comfort: avoiding overheating in European buildings, 2013.
[30] C.M. Smith, Technical knockout, Science 14 (2000) 32.